

Fractional topological liquids with time-reversal symmetry and their lattice realization

Titus Neupert,¹ Luiz Santos,² Shinsei Ryu,³ Claudio Chamon,⁴ and Christopher Mudry¹

¹*Condensed matter theory group, Paul Scherrer Institute, CH-5232 Villigen PSI, Switzerland*

²*Department of Physics, Harvard University, 17 Oxford St., Cambridge, MA 02138*

³*Department of Physics, University of California, Berkeley, CA 94720, USA*

⁴*Physics Department, Boston University, Boston, MA 02215, USA*

(Dated: March 25, 2025)

We present a class of time-reversal-symmetric fractional topological liquid states in two dimensions that support fractionalized excitations. These are incompressible liquids made of electrons, for which the charge Hall conductance vanishes and the spin Hall conductance need not be quantized. We then analyze the stability of edge states in these two-dimensional topological fluids against localization by disorder. We find a \mathbb{Z}_2 stability criterion for whether or not there exists a Kramers pair of edge modes that is robust against disorder. We also introduce an interacting electronic two-dimensional lattice model based on partially filled flattened bands of a \mathbb{Z}_2 topological band insulator, which we study using numerical exact diagonalization. We show evidence for instances of the fractional topological liquid phase as well as for a time-reversal symmetry broken phase with a quantized (charge) Hall conductance in the phase diagram for this model.

I. INTRODUCTION

The hallmark of the integer quantum effect (IQHE) in an open geometry is the localized nature of all two-dimensional (bulk) states while an integer number of chiral edge states freely propagate along the one-dimensional boundaries.^{1–3} These chiral edge states are immune to the physics of Anderson localization as long as backward scattering between edge states of opposite chiralities is negligible.^{2,3}

Many-body interactions among electrons can be treated perturbatively in the IQHE provided the characteristic many-body energy scale is less than the single-particle gap between Landau levels. This is not true anymore if the chemical potential lies within a Landau level as the non-interacting many-body ground state is then macroscopically degenerate. The lifting of this extensive degeneracy by the many-body interactions is a non-perturbative effect. At some “magic” filling fractions that deliver the fractional quantum Hall effect (FQHE),^{4–7} a screened Coulomb interaction selects a finitely degenerate family of ground states, each of which describes a featureless liquid separated from excitations by an energy gap in a closed geometry. Such a ground state is called an incompressible fractional Hall liquid. The FQHE is an example of topological order.⁸ In an open geometry, there are branches of excitations that disperse across the spectral gap of the two-dimensional bulk, but these excitations are localized along the direction normal to the boundary while they propagate freely along the boundary.^{9–11} Contrary to the IQHE, these excitations need not all share the same chirality. However, they are nevertheless immune to the physics of Anderson localization provided scattering induced by the disorder between distinct edges in an open geometry is negligible.

The integer quantum Hall effect (IQHE) is the archetype of a two-dimensional topological band insulator. The two-dimensional \mathbb{Z}_2 topological band insulator is a close relative of the IQHE that occurs in semi-

conductors with sufficiently large spin-orbit coupling but no breaking of time-reversal symmetry.^{12–16} As with the IQHE, the smoking gun for the \mathbb{Z}_2 topological band insulator is the existence of gapless Kramers degenerate pairs of edge states that are delocalized along the boundaries of an open geometry as long as disorder-induced scattering between distinct boundaries is negligible. In contrast to the IQHE, it is the odd parity in the number of Kramers pairs of edge states that is robust to the physics of Anderson localization.

A simple example of a two-dimensional \mathbb{Z}_2 topological band insulator can be obtained by putting together two copies of an IQHE system with opposite chiralities for up and down spins. For instance, one could take two copies of Haldane’s model,¹⁷ each of which realizes an integer Hall effect on the honeycomb lattice, but with Hall conductance differing by a sign. In this case the spin current is conserved, a consequence of the independent conservation of the up and down currents, and the spin Hall conductance inherits its quantization from the IQHE of each spin species. This example thus realizes an integer quantum spin Hall effect (IQSHE). However, although simple, this example is not generic. The \mathbb{Z}_2 topological band insulator does not necessarily have conserved spin currents, let alone quantized responses.

Along the same line of reasoning, two copies of a FQHE system put together, again with opposite chiralities for up and down particles, would realize a fractional quantum spin Hall effect (FQSHE), as proposed by Bernevig and Zhang.¹⁴ (See also Refs. 18 and 19.) Levin and Stern in Ref. 20 proposed to characterize two-dimensional fractional topological liquids supporting the FQSHE by the criterion that their edge states are stable against disorder provided that they do not break time-reversal symmetry spontaneously.

In this paper, we shall *not* impose the condition that projection about some quantization axis of the electron spin from the underlying microscopic model is a good quantum number. We will only demand that time-

reversal symmetry holds. We shall thus distinguish the generic cases of fractional topological liquids with time-reversal symmetry from the special cases of fractional topological liquids with time-reversal symmetry *and* with residual spin-1/2 U(1) rotation symmetry. In the former cases, the electronic spin is not a good quantum number. In the latter cases, conservation of spin allows for the FQSHE.

The subclass of incompressible time-reversal-symmetric liquids that we construct here is closely related to Abelian Chern-Simons theories. Other possibilities that are not discussed in this publication, may include non-Abelian Chern Simons theories,^{21,22} or theories that include, additionally, conventional local order parameters (Higgs fields).²³

The relevant effective action for the Abelian Chern-Simons theory is of the form⁹⁻¹¹

$$S := \int dt d^2\mathbf{x} \epsilon_{\mu\nu\rho} \left(\frac{1}{4\pi} K_{ij} a_\mu^i \partial_\nu a_\rho^j + \frac{e}{2\pi} Q_i A_\mu \partial_\nu a_\rho^i \right). \quad (1.1a)$$

The indices i, j run from 1 to $2N$ and any pair thereof labels an integer-valued matrix element K_{ij} of the symmetric and invertible $2N \times 2N$ matrix K . The indices μ, ν, ρ run from 0 to 2, they either label the component, say $A_\mu(t, \mathbf{x})$, of an electromagnetic gauge potential in (2+1)-dimensional space and time or the components of $2N$ flavors of Chern-Simons fields, say $a_\mu^i(t, \mathbf{x})$. The integer-valued component Q_i of the $2N$ -dimensional vector Q represents the i -th electric charge in units of the electronic charge e and obeys the compatibility condition

$$(-)^{Q_i} = (-)^{K_{ii}} \quad (1.1b)$$

for any $i = 1, \dots, 2N$ in order for bulk quasiparticles or, in an open geometry, quasiparticles on edges to obey a consistent statistics. The operation of time reversal maps $a_\mu^i(t, \mathbf{x})$ into $-\eta^{\mu\nu} a_\nu^{i+N}(-t, \mathbf{x})$ for $i = 1, \dots, N$ and vice versa. Here, $\eta_{\mu\nu} = \text{diag}(+, -, -)$ is the Lorentz metric. We will show that time-reversal symmetry imposes that the matrix K is of the block form

$$K = \begin{pmatrix} \kappa & \Delta \\ \Delta^\top & -\kappa \end{pmatrix}, \quad (1.2a)$$

$$\kappa^\top = \kappa, \quad \Delta^\top = -\Delta, \quad (1.2b)$$

where κ and Δ are $N \times N$ matrices, while the integer-charge vector Q is of the block form

$$Q = \begin{pmatrix} \varrho \\ \varrho \end{pmatrix}. \quad (1.2c)$$

The K matrix and charge vector Q that characterize the topological field theory with the action (1.1a) define the filling fraction, a rational number,

$$\nu := Q^\top K^{-1} Q. \quad (1.3a)$$

The block forms of K and Q in Eq. (1.2) imply that

$$\nu = 0. \quad (1.3b)$$

The “zero filling fraction” (1.3) states nothing but the fact that there is no charge Hall conductance when time-reversal symmetry holds. The special cases of the FQSHE treated in Refs. 14 and 20 correspond to imposing the condition

$$\Delta = 0 \quad (1.4)$$

on the K matrix in Eq. (1.2a). This restriction is, however, not necessary to treat either the FQSHE or the generic case when there is no residual spin-1/2 U(1) symmetry in the underlying microscopic model.

The effective topological field theory (1.1) with the condition for time-reversal symmetry (1.2) is made of $2N$ Abelian Chern-Simons fields. As is the case with the FQHE, when two-dimensional space is a closed manifold with genus one, i.e., when two-dimensional space is topologically equivalent to a torus, it is characterized by distinct topological sectors. All topological sectors are in one-to-one correspondence with a finite number \mathcal{N}_{GS} of topologically degenerate ground states of the underlying microscopic theory. This degeneracy is nothing but the magnitude of the determinant K in Eq. (1.1a), which is, because of the block structure (1.2a), in turn given by

$$\begin{aligned} \mathcal{N}_{\text{GS}} &= \left| \det \begin{pmatrix} \kappa & \Delta \\ \Delta^\top & -\kappa \end{pmatrix} \right| \\ &= \left| \det \begin{pmatrix} \Delta^\top & -\kappa \\ \kappa & \Delta \end{pmatrix} \right| \\ &= \left| \text{Pf} \begin{pmatrix} \Delta^\top & -\kappa \\ \kappa & \Delta \end{pmatrix} \right|^2 \\ &= (\text{integer})^2. \end{aligned} \quad (1.5)$$

To reach the last line we made use of the fact that the K matrix is integer valued. We thus predict that the class of two-dimensional time-reversal-symmetric fractional topological liquids, whose universal properties are captured by Eqs. (1.1) and (1.2), are characterized by a topological ground state degeneracy that is always the square of an integer, even if $\Delta \neq 0$, when space is topologically equivalent to a torus. (Notice that the condition that Δ is anti-symmetric implies that non-vanishing Δ can only occur for $N > 1$.)

We discuss in detail the stability of the edge states associated with the bulk Chern-Simons action (1.1) obeying the condition for the time-reversal symmetry (1.2). We consider a single one-dimensional edge and construct an interacting quantum field theory for $1 \leq N_K \leq N$ pairs of Kramers degenerate electrons subject to strong disorder that preserves time-reversal symmetry. (The integer $2N_K$ is the number of odd charges entering the charge vector Q .²⁴) We identify the conditions under which at least one Kramers degenerate pair of electrons remains gapless in spite of the interactions and disorder. Our approach is here inspired by the stability analysis of the edge states performed for the single-layer FQHE by Haldane in Ref. 25 (see also Refs. 26 and 27), by Naud et al. in Refs. 28 and 29 for the bilayer FQHE, and specially

that by Levin and Stern in Ref. 20 for the FQSHE. As for the FQSHE, our analysis departs from the analysis of Haldane in that we impose time-reversal symmetry. In this paper, we also depart from Ref. 20 by considering explicitly the effects of the off-diagonal elements Δ in the K -matrix. Such terms are generically present for any realistic underlying microscopic model independently of whether this underlying microscopic model supports or not the FQSHE. When considering the stability of the edge theory, we allow the residual spin-1/2 $U(1)$ symmetry responsible for the FQSHE to be broken by interactions among the edge modes or by a disorder potential. Hence, we seek a criterion for the stability of the edge theory that does not rely on the existence of a quantized spin Hall conductance in the bulk as was done in Ref. 20.

The stability of the edge states against disorder hinges on whether the integer

$$R := r \varrho^\top (\kappa - \Delta)^{-1} \varrho \quad (1.6)$$

is odd (stable) or even (unstable). The vector ϱ together with the matrices κ and Δ were defined in Eq. (1.2). The integer r is the smallest integer such that all the N components of the vector $r(\kappa - \Delta)^{-1} \varrho$ are integers. We can quickly check a few simple examples. First, observe that, in the limit $\Delta = 0$, we recover the criterion derived in Ref. 20. Second, when we impose a residual spin-1/2 $U(1)$ symmetry by appropriately restricting the interactions between edge channels, $\nu_\uparrow = -\nu_\downarrow = \varrho^\top (\kappa - \Delta)^{-1} \varrho$ can be interpreted as the Hall conductivity σ_{xy} in units of e^2/h for each of the separately conserved spin components along the spin quantization axis. The integer r has the interpretation of the number of fluxes needed to pump a unit of charge, or the inverse of the “minimum charge” of Ref. 20. Further restricting to the case when $\kappa = \mathbb{1}_N$ gives $R = N$, i.e., we have recovered the same criterion as for the two-dimensional non-interacting \mathbb{Z}_2 topological band insulator.

When there is no residual spin-1/2 $U(1)$ symmetry, one can no longer relate the index R to a physical spin Hall conductance. Nevertheless, the index R defined in Eq. (1.6) discriminates in all cases whether there is or not a remaining branch of gapless modes dispersing along the edge.

Before we turn to the detailed analysis of the stability of the edge theory in Sec. III, we shall first pose and answer the question of whether one can realize examples of the Abelian Chern-Simons subclass of time-reversal-symmetric topological spin states in a two-dimensional lattice model in Sec. II. We construct extensions of the lattice models studied in Refs. 30, 31, 32, and 33 for which a FQHE was found by partially filling flat bands with non-trivial Chern numbers, as proposed in Refs. 30, 34, and 35. (See also Ref. 36 for a discussion of isolated flat bands with broken time-reversal symmetry in two-dimensional lattices; Refs. 37 and 38 for recent progress on the understanding of the relations between Chern and Landau bands; and Ref. 39 for predicting that materials belonging to the family of heterostructures of transition-

metal oxides, say LaAuO_3 , might realize time-reversal symmetric topologically non-trivial band insulators with nearly flat bands.)

The systems studied here start with flat bands that realize at half-filling a two-dimensional integer quantum spin Hall band insulator. We study with the help of exact diagonalization the nature of the ground state selected by interactions at partial filling $2/3$ of the lowest band. We find supporting evidences for a featureless ground state that is consistent with the existence of a spectral gap and a topological degeneracy 3^2 in the thermodynamic limit, associated with a $\Delta = 0$ state, i.e., a FQSHE driven by interactions in a region of the phase diagram. This state is unstable to spontaneous symmetry breaking of time-reversal symmetry induced by sufficiently strong interactions, which lands the system onto a state with degeneracy 3 (not the square of an integer), which we identify with a $1/3$ FQHE of a magnetized state.

We close this paper with a summary in Sec. IV. We also include two appendices to render the paper reasonably self-contained.

II. EXACT DIAGONALIZATION STUDY OF A TWO-DIMENSIONAL LATTICE MODEL WITH TIME-REVERSAL SYMMETRY

In Sec. III, we will pose and answer the following question: Given a time-reversal-symmetric incompressible liquid-like ground state whose universal properties are encoded by a low-energy and long-wavelength effective quantum field theory for $2N$ Abelian Chern-Simons fields, under what conditions is a Kramers pair of edge modes that propagates at the boundary protected against Anderson localization as long as time-reversal symmetry is preserved. In this Section, we want to address the question, if and when such a posited topological state emerges in the first place. If an incompressible state is connected to a translation invariant band insulator, once interactions are switched off adiabatically, the answer is entirely governed by the Bloch states of the single-particle Hamiltonian and is well understood.^{40–42} If, however, the incompressibility of the state emerges from the interactions, the problem is qualitatively different.

As a starting point to study the latter situation, we shall follow the approach of Refs. 14 and 20 and consider two decoupled copies of the same incompressible fractional quantum Hall (FQH) state to compose an incompressible time-reversal symmetric fractional quantum spin Hall (FQSH) state from them. Then, we know that the ground state of the system is the direct product of the two FQH states and thus it is also an incompressible liquid. It is then natural to ask how stable this state is when the two FQH states are coupled, i.e., whether interactions *between* the two FQH states are (i) destroying the incompressibility, (ii) breaking spontaneously time-reversal symmetry, or (iii) generating other incompressible time-reversal symmetric states that are not captured

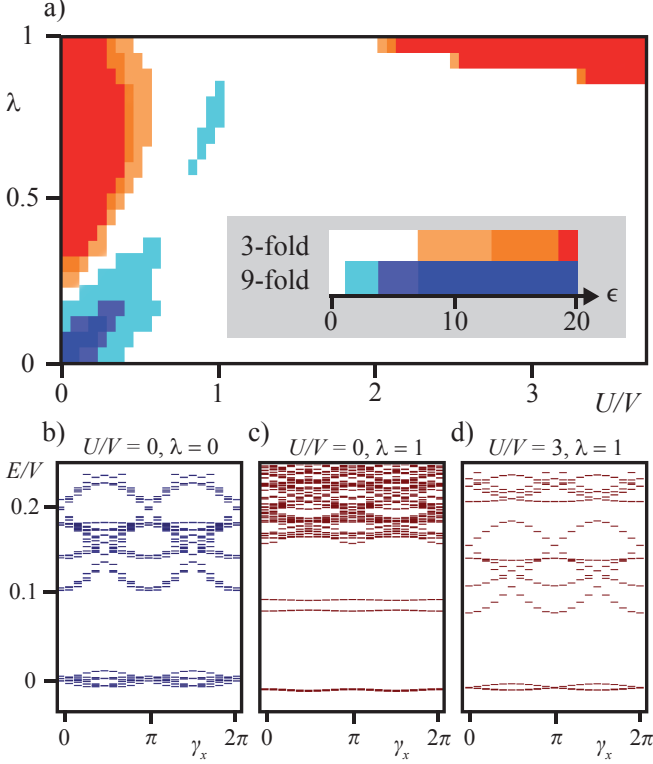


FIG. 1. (color online). Numerical exact diagonalization results of Hamiltonian (2.1) for 16 electrons when sublattice A is made of 3×4 sites and with $t_2/t_1 = 0.4$. (a) Ground state degeneracies. Denote with E_n the n -th lowest energy eigenvalue of the many-body spectrum where E_1 is the many-body ground state, i.e., $E_{n+1} \geq E_n$ for $n = 1, 2, \dots$. Define the parameter ϵ by $\epsilon_n := (E_{n+1} - E_n)/(E_n - E_1)$. If a large gap $E_{n+1} - E_n$ opens up between two consecutive levels E_{n+1} and E_n compared to the cumulative level splitting $E_n - E_1$ between the first n many-body eigenstates induced by finite-size effects, then the parameter ϵ_n is much larger than unity. The parameter ϵ_n has been evaluated for $n = 3$ and $n = 9$, yielding the blue and red regions, respectively. For all other $n \neq 1$, no regions with $\epsilon_n \gtrsim O(1)$ of significant size were found. Within the limited range of available system sizes, it is thus not possible to decide on whether and how the level-splitting above the ground state in the white regions of the parameter space extrapolates in the thermodynamic limit. (b)-(d) The lowest eigenvalues with spin-dependent twisted boundary conditions as a function of the twisting angle γ_x . The number of low-lying states that are energetically separated from the other states is 9, 3, and 3, respectively. In panel (c), it is the lowest band parametrized by γ_x that is 3-fold degenerate.

by the Abelian Chern-Simons theory in Eq. (1.1).

We are going to address this question by numerical exact diagonalization of an interacting lattice model, where we will find evidence for all scenarios (i), (ii), and (iii). It is advantageous to consider a system in which the z -component of the electronic spin is conserved, i.e., with a residual spin-1/2 U(1) symmetry. This makes larger system sizes accessible and allows to study the model with spin-dependent twisted boundary conditions in order to

determine the ground-state degeneracy as explained below. We consider spinfull electrons hopping on the square lattice $\Lambda = A \cup B$ made up of the two sublattices A and B. The Hamiltonian

$$H = H_0 + H_{\text{int}} \quad (2.1)$$

decomposes into a quadratic part H_0 and an interacting contribution H_{int} .

First, let us define H_0 , which consists of two copies of the π -flux phase with flat bands that was studied in Ref. 30, one copy for each spin-1/2 species. We denote with $c_{\mathbf{k},\alpha,\sigma}^\dagger$ the creation operator for an electron with lattice momentum \mathbf{k} and spin $\sigma = \uparrow, \downarrow$ in the sublattice $\alpha = A, B$ and combine them in the sublattice-spinor $\psi_{\mathbf{k},\sigma}^\dagger := (c_{\mathbf{k},A,\sigma}^\dagger, c_{\mathbf{k},B,\sigma}^\dagger)$. Then, the second quantized single-particle Hamiltonian reads

$$H_0 := \sum_{\mathbf{k} \in \text{BZ}} \left(\psi_{\mathbf{k},\uparrow}^\dagger \frac{\mathbf{B}_{\mathbf{k}} \cdot \boldsymbol{\tau}}{|\mathbf{B}_{\mathbf{k}}|} \psi_{\mathbf{k},\uparrow} + \psi_{\mathbf{k},\downarrow}^\dagger \frac{\mathbf{B}_{-\mathbf{k}} \cdot \boldsymbol{\tau}^\top}{|\mathbf{B}_{-\mathbf{k}}|} \psi_{\mathbf{k},\downarrow} \right), \quad (2.2a)$$

where the 3-vector $\mathbf{B}_{\mathbf{k}}$ is defined by

$$B_{0,\mathbf{k}} := 0, \quad (2.2b)$$

$$B_{1,\mathbf{k}} + iB_{2,\mathbf{k}} := t_1 e^{-i\pi/4} \left(1 + e^{+i(k_y - k_x)} \right) + t_1 e^{+i\pi/4} \left(e^{-ik_x} + e^{+ik_y} \right), \quad (2.2c)$$

$$B_{3,\mathbf{k}} := 2t_2 (\cos k_x - \cos k_y), \quad (2.2d)$$

and the three Pauli-matrices $\boldsymbol{\tau} = (\tau_1, \tau_2, \tau_3)$ act on the sublattice index. Here, t_1 and t_2 represent the nearest neighbor (NN) and next-nearest neighbor (NNN) hopping amplitudes. The Hamiltonian (2.2a) is only well defined if $t_2 \neq 0$.

One verifies that H_0 is both time-reversal symmetric and invariant under spin-1/2 U(1) rotations. Indeed, the time-reversal operation \mathcal{T} acts on numbers as complex conjugation and on the electron-operators as

$$\psi_{\mathbf{k},\uparrow}^\dagger \xrightarrow{\mathcal{T}} +\psi_{-\mathbf{k},\downarrow}^\dagger, \quad \psi_{\mathbf{k},\downarrow}^\dagger \xrightarrow{\mathcal{T}} -\psi_{-\mathbf{k},\uparrow}^\dagger. \quad (2.3)$$

The action of the spin-1/2 U(1) rotation \mathcal{R}_γ by the angle $0 \leq \gamma < 2\pi$ is given by

$$\psi_{\mathbf{k},\uparrow}^\dagger \xrightarrow{\mathcal{R}_\gamma} e^{+i\gamma} \psi_{\mathbf{k},\uparrow}^\dagger, \quad \psi_{\mathbf{k},\downarrow}^\dagger \xrightarrow{\mathcal{R}_\gamma} e^{-i\gamma} \psi_{\mathbf{k},\downarrow}^\dagger. \quad (2.4)$$

The spectrum of H_0 is gaped and comprises four dispersionless bands with the energy-eigenvalues

$$\varepsilon_{\mathbf{k},\sigma,\pm} = \pm 1, \quad \sigma = \uparrow, \downarrow. \quad (2.5)$$

Denoting the corresponding single-particle eigenstates by $\chi_{\mathbf{k},\sigma,\pm}$, $\sigma = \uparrow, \downarrow$, we can define the spin-resolved first Chern numbers for each of the two pairs of degenerate single-particle bands as

$$C_{s,\pm} := \frac{1}{2} \int_{\mathbf{k} \in \text{BZ}} \frac{d^2 \mathbf{k}}{2\pi i} \nabla_{\mathbf{k}} \wedge \left(\chi_{\mathbf{k},\uparrow,\pm}^\dagger \nabla_{\mathbf{k}} \chi_{\mathbf{k},\uparrow,\pm} - \chi_{\mathbf{k},\downarrow,\pm}^\dagger \nabla_{\mathbf{k}} \chi_{\mathbf{k},\downarrow,\pm} \right). \quad (2.6)$$

We find $C_{s,\pm} = \pm 1$. As a consequence, the non-interacting model exhibits an IQSHE with spin-Hall conductivity $\sigma_{xy}^{\text{SH}} = 2 \times e/(4\pi)$ if the chemical potential lies in the single-particle spectral gap.

The repulsive interactions in this model are defined by

$$H_{\text{int}} := U \sum_{i \in \Lambda} \rho_{i,\uparrow} \rho_{i,\downarrow} + V \sum_{\langle ij \rangle \in \Lambda} \left[\rho_{i,\uparrow} \rho_{j,\uparrow} + \rho_{i,\downarrow} \rho_{j,\downarrow} + \lambda (\rho_{i,\uparrow} \rho_{j,\downarrow} + \rho_{i,\downarrow} \rho_{j,\uparrow}) \right], \quad (2.7)$$

where $\langle ij \rangle$ are directed NN bonds of the square lattice $\Lambda = \text{A} \cup \text{B}$, $\rho_{i,\sigma}$ is the occupation number of the site i with electrons of spin σ . The interacting Hamiltonian H_{int} comprises an on-site Hubbard term with the coupling $U \geq 0$ and a NN term which is parametrized by the coupling $V > 0$ and the dimensionless number $\lambda \in [0, 1]$. The value $\lambda = 1$ corresponds to the spin-1/2 SU(2)-symmetric limit, while all other values of λ correspond to the spin-1/2 U(1)-symmetric limit. These interactions lift the macroscopic degeneracy of the single-particle bands. They couple the spin-up and the spin-down sector, if at least one of U or λ is non-vanishing. Notice that H_{int} shares both the time-reversal and spin-1/2 U(1) symmetries of the single-particle Hamiltonian H_0 .

Periodic boundary conditions are imposed on lattice Λ whereby sublattice A contains $L_x \times L_y$ sites. We fix the number of electrons to be 16 while $L_x = 3$ and $L_y = 4$. We define the filling fraction $2/3$ to be the number of particles, 16, divided by the number of Bloch single-particle states in the lowest spin-degenerate band, $(3 \times 4 \times 2 \times 2)/2 = 48/2 = 24$. We then project Hamiltonian (2.1) onto the states in the two lower single-particle bands $\varepsilon_{\mathbf{k},\uparrow,-}$, $\varepsilon_{\mathbf{k},\downarrow,-}$, thereby assuming that the single-particle gap is much larger than the energy scale of the interactions. Exact diagonalization yields the many-body spectrum as a function of the interaction parameters λ and U/V . We identify three distinct incompressible states in the $\lambda - U$ phase diagram [see Fig. 1(a)].

Case $\lambda = U/V = 0$: decoupled FQH states — The model decouples into two FQH-like states at $2/3$ filling, one for each spin orientation. The low-energy effective theory for this state is characterized by the K matrix

$$K = \begin{pmatrix} +1 & +2 & 0 & 0 \\ +2 & +1 & 0 & 0 \\ 0 & 0 & -1 & -2 \\ 0 & 0 & -2 & -1 \end{pmatrix}, \quad Q = \begin{pmatrix} 1 \\ 1 \\ 1 \\ 1 \end{pmatrix}, \quad (2.8)$$

and has degeneracy $\det K = 3^2 = 9$ as confirmed by the numerical results. This phase is destabilized by introducing a sufficiently strong coupling between the two FQH states via λ and U . The ability to make a quantitative statement on the boundary of this phase in the phase diagram is here limited by the difficulty in deciding on the compressibility of a state from extrapolation of exact diagonalization studies of small systems sizes to the thermodynamic limit.

Case $\lambda = 1, U/V > 2$: Spontaneous symmetry breaking — We observe that the ground state has the maximal spin-polarization that is allowed by the Pauli principle. To interpret this numerical result, first recall that, after projection onto the lowest bands, at most $L_x \times L_y$ electrons may have the same spin, i.e., 12 for the case at hand. Now, the filling fraction is $2/3$, i.e., there are $4/3 \times L_x \times L_y = 16$ electrons. If 12 electrons are fully spin polarized, which is what we observe numerically, then the remaining $1/3 \times L_x \times L_y = 4$ electrons may form a $1/3$ FQH-like state. We conjecture that the low-energy effective theory for this fully spin-polarized ground state is characterized by the K matrix

$$K = \begin{pmatrix} +1 & 0 \\ 0 & -3 \end{pmatrix}, \quad Q = \begin{pmatrix} 1 \\ 1 \end{pmatrix} \quad (2.9a)$$

with the filling fraction

$$\nu = Q^T K^{-1} Q = 2/3. \quad (2.9b)$$

Clearly, this K -matrix does not obey the decomposition (1.2), since time-reversal symmetry is spontaneously broken. The degeneracy $|\det K| = 3$ is confirmed by the numerical results. The state thus obtained resembles the conventional double-layer $2/3$ FQH state, with the difference that the electron spins are not fully polarized.

Case $\lambda = 1, U/V = 0$: Possible paired state — A time-reversal symmetric state with a spectral gap and a 3-fold ground state degeneracy is obtained for small U/V . This state cannot be captured by the Abelian Chern-Simons theory in Eq. (1.1), since its degeneracy is not the square of an integer, despite the time-reversal symmetry. One may speculate that this state realizes some real-space pairing of spin-up with spin-down electrons, since for small U/V it costs little energy to have two electrons of opposite spin at the same lattice site.

We close Sec. II with some technical material. To determine the degeneracy of the ground state unambiguously, we have used spin-dependent twisted boundary conditions along the x -direction defined by

$$\langle \mathbf{r} + L_x \hat{\mathbf{x}} | \Psi_{\gamma_x} \rangle = \langle \mathbf{r} | e^{i\gamma_x \sigma_3} | \Psi_{\gamma_x} \rangle, \quad (2.10)$$

where Ψ_{γ_x} is the many-body state, σ_3 acts on the spin degrees of freedom, and $\hat{\mathbf{x}}$ is the corresponding basis vector of the lattice. Imposing this boundary condition is equivalent to inserting the flux γ_x and its time-reversed flux $-\gamma_x$ for electrons with spin up and spin down quantum numbers, respectively. This is a well-defined operation due to the residual spin-1/2 U(1) symmetry that preserves time-reversal symmetry for any value of γ_x . For the three cases discussed above, Fig. 1(b-d) shows that the states of the (nearly degenerate) ground-state manifold remain well separated from the continuum of states as γ_x is varied from 0 to 2π , thereby confirming the 9-fold and 3-fold degeneracy, respectively.

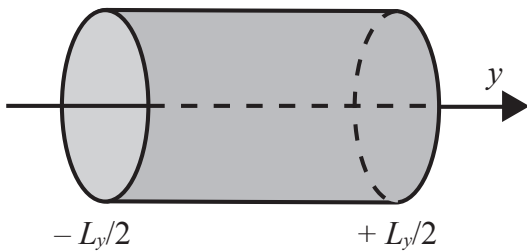


FIG. 2. Cylindrical geometry for a two-dimensional band insulator. The cylinder axis is labeled by the co-ordinate y . Periodic boundary conditions are imposed in the transverse direction labeled by the co-ordinate x . There is an edge at $y = -L_y/2$ and another one at $y = +L_y/2$. Bulk states have a support on the shaded surface of the cylinder. Edge states are confined in the y direction to the vicinity of the edges $y = \pm L_y/2$. Topological band insulators have the property that there are edge states freely propagating in the x direction even in the presence of disorder with the mean free path ℓ provided the limit $\ell/L_y \ll 1$ holds.

III. EDGE THEORY WITH TIME-REVERSAL SYMMETRY

We consider an interacting model for electrons in a two-dimensional cylindrical geometry as is depicted in Fig. 2. We demand that (i) charge conservation and time-reversal symmetry are the only intrinsic symmetries of the microscopic quantum Hamiltonian, (ii) neither are broken spontaneously by the many-body ground state, and (iii), if periodic boundary conditions are assumed along the y co-ordinate in Fig. 2, then there is at most a finite number of degenerate many-body ground states and each many-body ground state is separated from its tower of many-body excited states by an energy gap. Had we relaxed the condition that time-reversal symmetry holds, the remaining assumptions would be realized for the FQHE.

In the open geometry of Fig. 2, the only possible excitations with an energy smaller than the bulk gap in the closed geometry of a torus must be localized along the y co-ordinate in the vicinities of the edges at $\pm L_y/2$. If L_y is much larger than the characteristic linear extension into the bulk of edge states, the two edges decouple from each other. It is then meaningful to define a low-energy and long-wavelength quantum field theory for the edge states propagating along any one of the two boundaries in Fig. 2, which we take to be of length L each.

The low-energy and long-wavelength effective quantum field theory for the edge that we are going to construct is inspired by the construction by Wen of the chiral Luttinger edge theory for the FQHE.^{9–11} As for the FQHE, this time-reversal symmetric boundary quantum field theory has a correspondence to the effective time-reversal symmetric bulk topological quantum-field theory built out of $2N$ Abelian Chern-Simon fields and defined by Eqs. (1.1) and (1.2).⁴³

The simplest class of quantum Hamiltonians that ful-

fills requirements (i)-(iii) can be represented in terms of $2N$ real-valued chiral scalar quantum fields $\hat{\Phi}_i(t, x)$ with $i = 1, \dots, 2N$ that form the components of the quantum vector field $\hat{\Phi}(t, x)$. After setting the electric charge e , the speed of light c , and \hbar to unity, the Hamiltonian for the system is given by

$$\hat{H} := \hat{H}_0 + \hat{H}_{\text{int}}, \quad (3.1a)$$

where

$$\hat{H}_0 := \int_0^L dx \frac{1}{4\pi} \partial_x \hat{\Phi}^\top V \partial_x \hat{\Phi}, \quad (3.1b)$$

with V a $2N \times 2N$ symmetric and positive definite matrix that accounts, in this bosonic representation, for the screened translation-invariant two-body interactions between electrons. The theory is quantized according to the equal-time commutators

$$[\hat{\Phi}_i(t, x), \hat{\Phi}_j(t, x')] = -i\pi \left(K_{ij}^{-1} \text{sgn}(x - x') + \Theta_{ij} \right) \quad (3.1c)$$

where K is a $2N \times 2N$ symmetric and invertible matrix with integer-valued matrix elements, and the Θ matrix accounts for Klein factors that ensure that charged excitations in the theory (vertex operators) satisfy the proper commutation relations. We review the construction of the vertex operators in detail in Appendix A. In particular, fermionic or bosonic charged excitations are represented by the normal ordered vertex operators

$$\hat{\Psi}_T^\dagger(t, x) := : e^{-i T_i K_{ij} \hat{\Phi}_j(t, x)} : , \quad (3.1d)$$

where the integer-valued $2N$ -dimensional vector T determines the charge (and statistics) of the operator. The operator that measures the total charge density is

$$\hat{\rho} = \frac{1}{2\pi} Q_i \partial_x \hat{\Phi}_i, \quad (3.1e)$$

where the integer-valued $2N$ -dimensional charge vector Q , together with the K -matrix, specify the universal properties of the edge theory. The charge q_T of the vertex operator in Eq. (3.1d) follows from its commutation with the charge density operator in Eq. (3.1e), yielding $q_T = T^\top Q$.

Tunneling of electronic charge among the different edge branches is accounted for by

$$\hat{H}_{\text{int}} := - \int_0^L dx \sum_{T \in \mathbb{L}} h_T(x) : \cos \left(T^\top K \hat{\Phi}(x) + \alpha_T(x) \right) : \quad (3.1f)$$

The real functions $h_T(x) \geq 0$ and $0 \leq \alpha_T(x) \leq 2\pi$ encode information about the disorder along the edge when position dependent. The set

$$\mathbb{L} := \{ T \in \mathbb{Z}^{2N} \mid T^\top Q = 0 \} \quad (3.1g)$$

encodes all the possible charge neutral tunneling processes, i.e., those that just rearrange charge among the branches. This charge neutrality condition implies that the operator $\hat{\Psi}_T^\dagger(t, x)$ is bosonic, for it has even charge. Observe that set \mathbb{L} forms a lattice. Consequently, if T belongs to \mathbb{L} so does $-T$. In turn, relabeling T to $-T$ in \hat{H}_{int} implies that $h_T(x) = +h_{-T}(x)$ whereas $\alpha_T(x) = -\alpha_{-T}(x)$. A discussion of the gauge symmetries of this model and the properties of \mathbb{L} can be found in Appendix A.

The theory (3.1) is inherently encoding interactions: The terms \hat{H}_0 and \hat{H}_{int} encode single-particle *as well as* many-body interactions with matrix elements that preserve and break translation symmetry, respectively. Recovering the single-particle kinetic energy of N Kramers degenerate pairs of electrons from Eq. (3.1b) corresponds to choosing the matrix V from to be proportional to the unit $2N \times 2N$ matrix with the proportionality constant fixed by the condition that the scaling dimension of each electron is $1/2$ at the bosonic free-field fixed point defined by Hamiltonian \hat{H}_0 . Of course, to implement the fermionic statistics for all $2N$ fermions, one must also demand that all diagonal entries of K are odd integers in some basis (see footnote 24). While we shall proceed with the interacting bosonic theory here, we complement this analysis with a review of the stability of N Kramers pairs of non-interacting fermions presented in Appendix B.

A. Time-reversal symmetry of the edge theory

The operation of time-reversal on the $\hat{\Phi}$ fields is defined by

$$\mathcal{T} \hat{\Phi}(t, x) \mathcal{T}^{-1} := \Sigma_1 \hat{\Phi}(-t, x) + \pi K^{-1} \Sigma_\downarrow Q, \quad (3.2a)$$

where

$$\Sigma_1 = \begin{pmatrix} 0 & \mathbb{1} \\ \mathbb{1} & 0 \end{pmatrix} \quad \text{and} \quad \Sigma_\downarrow = \begin{pmatrix} 0 & 0 \\ 0 & \mathbb{1} \end{pmatrix}. \quad (3.2b)$$

This definition ensures that fermionic and bosonic vertex operators as in Eq. (3.1d) are properly transformed under time reversal. More precisely, one can then construct a pair of fermionic operators $\hat{\Psi}_1^\dagger$ and $\hat{\Psi}_2^\dagger$ of the form (3.1d) by suitably choosing a pair of vectors T_1 and T_2 , respectively, in such a way that the operation of time-reversal maps $\hat{\Psi}_1^\dagger$ into $+\hat{\Psi}_2^\dagger$ whereas it maps $\hat{\Psi}_2^\dagger$ into $-\hat{\Psi}_1^\dagger$. Thus, it is meaningful to interpret the block structure displayed in Eq. (3.2b) as arising from the upper or lower projection along some spin-1/2 quantization axis.

Time-reversal symmetry on the chiral edge theory (3.1) demands the following conditions, that we explain below:

$$V = +\Sigma_1 V \Sigma_1, \quad (3.3a)$$

$$K = -\Sigma_1 K \Sigma_1, \quad (3.3b)$$

$$Q = \Sigma_1 Q, \quad (3.3c)$$

$$h_T(x) = h_{\Sigma_1 T}(x), \quad (3.3d)$$

$$\alpha_T(x) = \left(-\alpha_{\Sigma_1 T}(x) + \pi T^\top \Sigma_\downarrow Q \right) \bmod 2\pi. \quad (3.3e)$$

The first two conditions – Eqs. (3.3a) and (3.3b) – follow from the requirement that \hat{H}_0 be time-reversal invariant. In particular, the decomposition (1.2) of K follows from Eq. (3.3b) and $K = K^\top$. The third condition – Eq. (3.3c) – states that the charge density is invariant under time reversal. In particular, the decomposition (1.2) of Q follows from Eq. (3.3c). Finally, $\mathcal{T} \hat{H}_{\text{int}} \mathcal{T}^{-1} = \hat{H}_{\text{int}}$ requires

$$\begin{aligned} \sum_{T \in \mathbb{L}} h_T(x) \cos \left(T^\top K \hat{\Phi}(t, x) + \alpha_T(x) \right) &= \sum_{T \in \mathbb{L}} \mathcal{T} \left[h_T(x) \cos \left(T^\top K \hat{\Phi}(t, x) + \alpha_T(x) \right) \right] \mathcal{T}^{-1} \\ &= \sum_{T \in \mathbb{L}} h_T(x) \cos \left(-(\Sigma_1 T)^\top K \hat{\Phi}(-t, x) + \alpha_T(x) - \pi T^\top \Sigma_\downarrow Q \right) \\ &= \sum_{T \in \mathbb{L}} h_{\Sigma_1 T}(x) \cos \left(-T^\top K \hat{\Phi}(-t, x) + \alpha_{\Sigma_1 T}(x) - \pi (\Sigma_1 T)^\top \Sigma_\downarrow Q \right) \\ &= \sum_{T \in \mathbb{L}} h_{\Sigma_1 T}(x) \cos \left(T^\top K \hat{\Phi}(-t, x) - \alpha_{\Sigma_1 T}(x) + \pi (\Sigma_1 T)^\top \Sigma_\downarrow Q \right), \end{aligned} \quad (3.4)$$

leading to the last two relations – Eqs. (3.3d) and (3.3e) – as the conditions needed to match the two trigonometric expansions.

Disorder parametrized by $h_T(x) = +h_{-T}(x)$ and $\alpha_T(x) = -\alpha_{-T}(x)$ and for which the matrix T obeys

$$\Sigma_1 T = -T \quad (3.5a)$$

and

$$T^\top \Sigma_\downarrow Q \text{ is an odd integer} \quad (3.5b)$$

cannot satisfy the condition (3.3e) for time-reversal symmetry. It is thus prohibited to enter \hat{H}_{int} in Eq. (3.1f), for it would break explicitly time-reversal symmetry otherwise. Moreover, we also prohibit any ground state that provides $\exp(iT^\top K \hat{\Phi}(t, x))$ with an expectation value when T satisfies Eq. (3.5), for it would break spontaneously time-reversal symmetry otherwise.

B. Pinning the edge fields with disorder potentials

Solving the interacting theory (3.1) is beyond the scope of this paper. What can be done, however, is to identify those fixed points of the interacting theory (3.1) that are pertinent to the question of whether or not some edge modes remain extended along the edge in the limit of strong disorder $h_T(x) \rightarrow \infty$ for all tunneling matrices $T \in \mathbb{L}$ entering the interaction (3.1f).

This question is related to the one posed and answered by Haldane in Ref. 25 for Abelian FQH states and which in the context of this paper would be: Given an interaction potential caused by *weak* disorder on the edges as defined by Hamiltonian (3.1f), what are the tunneling vectors $T \in \mathbb{L}$ that can, in principle, describe relevant perturbations that will cause the system to flow to a strong coupling fixed point characterized by $h_T \rightarrow \infty$ away from the fixed point \hat{H}_0 ? (See Ref. 44 for an answer to this weak-coupling question in the context of the IQSHE and \mathbb{Z}_2 topological band insulators.) By focusing on the strong coupling limit from the outset, we avoid the issue of following the renormalization group flow from weak to strong coupling. Evidently, this point of view presumes that the strong coupling fixed point is stable and that no intermediary fixed point prevents it from being reached.

In order to identify the fixed points of the interacting theory (3.1) in the strong coupling limit (strong disorder limit) $h_T \rightarrow \infty$, we ignore the contribution \hat{H}_0 and

restrict the sum over the tunneling matrices in \hat{H}_{int} to a subset \mathbb{H} of \mathbb{L} ($\mathbb{H} \subset \mathbb{L}$) with a precise definition of \mathbb{H} that will follow in Eq. (3.10). For any choice of \mathbb{H} , there follows the strong-coupling fixed point Hamiltonian

$$\hat{H}_{\mathbb{H}} := - \int_0^L dx \sum_{T \in \mathbb{H}} h_T(x) : \cos \left(T^\top K \hat{\Phi}(x) + \alpha_T(x) \right) : . \quad (3.6)$$

We conjecture that a fixed point Hamiltonian (3.6) is stable if and only if the set \mathbb{H} is “maximal”. The study of the renormalization group flows relating the weak, moderate (if any), and the strong fixed points in the infinite-dimensional parameter space spanned by the non-universal data V , $h_T(x)$, and $\alpha_T(x)$ is again beyond the scope of this paper.

The reader might wonder why we cannot simply choose $\mathbb{H} = \mathbb{L}$. This is a consequence of the chiral equal-time commutation relations (3.1c), as emphasized by Haldane in Ref. 25, that prevent the simultaneous locking of the phases of all the cosines through

$$\partial_x \left(T^\top K \hat{\Phi}(t, x) + \alpha_T(x) \right) = C_T(x) , \quad (3.7)$$

for some time independent real-valued function $C_T(x)$. Even in the strong-coupling limit, there are quantum fluctuations as a consequence of the chiral equal-time commutation relations (3.1c) that prevent minimizing the interaction \hat{H}_{int} by minimizing separately each contribution to the trigonometric expansion (3.1f). Finding the ground state in the strong coupling limit is a strongly frustrated problem of optimization.

To construct a maximal set \mathbb{H} , we demand that any $T \in \mathbb{H}$ must satisfy the locking condition (3.7). Furthermore, we require that the phases of the cosines entering the fixed point Hamiltonian (3.6) be constants of motion

$$\left[\partial_x \left(T^\top K \hat{\Phi}(t, x) \right), \hat{H}_{\mathbb{H}} \right] = 0 . \quad (3.8)$$

In order to find the tunneling vectors $T \in \mathbb{H}$, we thus need to consider the following commutator

$$\left[\partial_x \left(T^\top K \hat{\Phi}(t, x) \right), h_{T'}(x) \cos \left(T'^\top K \hat{\Phi}(t, x') + \alpha_{T'}(x') \right) \right] = -i 2\pi T^\top K T' h_{T'}(x) \sin \left(T'^\top K \hat{\Phi}(t, x') + \alpha_{T'}(x') \right) \quad (3.9)$$

and demand that it vanishes. This is achieved if $T^\top K T' = 0$. Equation (3.9) implies that any set \mathbb{H} is composed of the charge neutral vectors satisfying $T^\top K T' = 0$. It is by choosing a set \mathbb{H} to be “maximal”

that we shall obtain the desired criterion for stability.

C. The stability criterion for edge modes

We presented and briefly discussed in the introduction (see Sec. I) the criteria for at least one branch of edge excitations to remain delocalized even in the presence of strong disorder. Here we prove these criteria. The idea is to count the maximum possible number of edge modes that can be pinned (localized) along the edge by tunneling processes. The set of pinning processes must satisfy

$$T^\top Q = 0 \quad \text{and} \quad T^\top K T' = 0, \quad (3.10)$$

which defines a set \mathbb{H} introduced in Sec. IIIB. (Note, however, that \mathbb{H} is not uniquely determined from this condition.) It is very useful to also define the real extension \mathbb{V} of a set \mathbb{H} , by allowing the tunneling vectors T that satisfy Eq. (3.10) to take real values instead of integer values. Notice that \mathbb{V} is a vector space over the real numbers. We shall also demand that \mathbb{H} forms a lattice that is as dense as the lattice \mathbb{L} by imposing

$$\mathbb{V} \cap \mathbb{L} = \mathbb{H}. \quad (3.11)$$

For any vector $T \in \mathbb{V}$, consider the vector KT . It follows from Eq. (3.10) that $KT \perp T', \forall T' \in \mathbb{V}$. So K maps the space \mathbb{V} into an orthogonal space \mathbb{V}^\perp . Since K is invertible, we have $\mathbb{V}^\perp = K\mathbb{V}$ as well as $\mathbb{V} = K^{-1}\mathbb{V}^\perp$, and thus $\dim \mathbb{V} = \dim \mathbb{V}^\perp$. Since $\dim \mathbb{V} + \dim \mathbb{V}^\perp \leq 2N$, it follows that $\dim \mathbb{V} \leq N$. Therefore (as could be anticipated physically) the maximum number of Kramers pairs of edge modes that can be pinned is N ; if that happens, the edge has no gapless delocalized mode.

Next, let us look at the conditions for which the maximum dimension N is achieved. If $\dim \mathbb{V} = \dim \mathbb{V}^\perp = N$, it follows that $\mathbb{V} \oplus \mathbb{V}^\perp = \mathbb{R}^{2N}$, exhausting the space of available vectors, and thus in this case the charge vector $Q \in \mathbb{V}^\perp$ because of Eq. (3.10). Consequently $K^{-1}Q \in \mathbb{V}$, and we can construct an integer vector $\bar{T} \parallel K^{-1}Q$ by scaling $K^{-1}Q$ by the minimum integer r that accomplishes this (which is possible because K^{-1} is a matrix with rational entries and Q is a vector of integers). Such a vector $\bar{T} \in \mathbb{H}$ is written as

$$\bar{T} := r \begin{pmatrix} +(\kappa - \Delta)^{-1} \varrho \\ -(\kappa - \Delta)^{-1} \varrho \end{pmatrix}. \quad (3.12)$$

The existence of $(\kappa - \Delta)^{-1}$ follows from $\det K \neq 0$ and

$$\det K = (-)^N [\det(\kappa - \Delta)]^2. \quad (3.13)$$

Using \bar{T} , we construct the integer

$$R := -\bar{T}^\top \Sigma_\downarrow Q, \quad (3.14)$$

which, as we argue below, determines if it is possible or not to localize all the modes with the N tunneling operators. Here we employ Eq. (3.3e), also noticing that

$\Sigma_1 \bar{T} = -\bar{T}$, and write

$$\begin{aligned} \pi R &= -\pi \bar{T}^\top \Sigma_\downarrow Q \\ &= \left(-\alpha_{\bar{T}}(x) - \alpha_{\Sigma_1 \bar{T}}(x) \right) \bmod 2\pi \\ &= \left(-\alpha_{\bar{T}}(x) - \alpha_{-\bar{T}}(x) \right) \bmod 2\pi \\ &= 0 \bmod 2\pi, \end{aligned} \quad (3.15)$$

where in the last line we used that $\alpha_T(x) = -\alpha_{-T}(x)$ for all $T \in \mathbb{L}$. If \bar{T} satisfies Eq. (3.15), then R must be an even integer. If Eq. (3.15) is violated, i.e., R is an odd integer, then \bar{T} is not allowed to enter \hat{H}_{int} for it would otherwise break time-reversal symmetry [thus $h_{\bar{T}}(x) = 0$ must always hold in this case in order to prevent \bar{T} from entering \hat{H}_{int}]. We therefore arrive at the condition that

- If the maximum number of edge modes are localized or gaped, then R must be even.

A corollary is that

- If R is odd, at least one edge branch is gapless and delocalized.

It remains for us to prove that if R is even, then one can indeed reach the maximum dimension N for the space of pinning vectors. This is done by construction. Take all eigenvectors of Σ_1 with $+1$ eigenvalue. We can take $(N-1)$ of such vectors, all those orthogonal to Q ; for the last one we take \bar{T} . One can check that these N vectors satisfy Eq. (3.10) with the help of $\Sigma_1 K \Sigma_1 = -K$ [listed in Eq. (3.3b)] and of $\bar{T} \parallel K^{-1}Q$. Now, the $(N-1)$ vectors $\Sigma_1 T = +T$ are of the form $T^\top = (t^\top, t^\top)$, where we need to satisfy $T^\top Q = 2t^\top \varrho = 0$. This leads to $T^\top \Sigma_\downarrow Q$ even, and then Eq. (3.3e) brings no further conditions whatsoever. So we can take all these $(N-1)$ tunneling vectors. Finally, we take \bar{T} as constructed above, which is a legitimate choice since R is assumed even and thus consistent with Eq. (3.15). Hence, we have constructed the N tunneling vectors that gap or localize all edge modes, and can state that

- If R is even, then the maximum number of edge modes are localized or gaped.

As a by-product, we see that it is always possible to localize along the boundary at least all but one Kramers degenerate pair of edge states via the $(N-1)$ tunneling vectors that satisfy $\Sigma_1 T = +T$. Thus, either one or no Kramers degenerate pair of edge state remains delocalized along the boundary when translation invariance is strongly broken along the boundary.

D. The stability criterion for edge modes in the FQSHE

What is the fate of the stability criterion when we impose the residual spin-1/2 $U(1)$ symmetry in the model so

as to describe an underlying microscopic model that supports the FQSHE? The residual spin-1/2 $U(1)$ symmetry is imposed on the interacting theory (3.1) by positing the existence of a spin vector $S = -\Sigma_1 S \in \mathbb{Z}^{2N}$ associated to a conserved $U(1)$ spin current. This spin vector is the counterpart to the charge vector $Q = +\Sigma_1 Q \in \mathbb{Z}^{2N}$. The condition

$$S = -\Sigma_1 S \quad (3.16a)$$

is required for compatibility with time-reversal symmetry and is the counterpart to Eq. (3.3c). Compatibility with time-reversal symmetry of Q and S thus imply that they are orthogonal, $Q^\top S = 0$. If we restrict the interaction (3.1f) by demanding that the tunneling matrices obey

$$T^\top S = 0, \quad (3.16b)$$

we probe the stability of the FQSHE described by \hat{H}_0 when perturbed by \hat{H}_{int} .⁴⁵

To answer this question we supplement the condition $T^\top Q = 0$ on tunneling vectors that belong to \mathbb{L} and \mathbb{H} , by $T^\top S = 0$. By construction, S is orthogonal to Q . Hence, it remains true that \mathbb{H} is made of at most N linearly independent tunneling vectors.

The strategy for establishing the condition for the strong coupling limit of \hat{H}_{int} to open a mobility gap for all the extended modes of \hat{H}_0 thus remains to construct the largest set \mathbb{H} out of as few tunneling vectors with $T = -\Sigma_1 T$ as possible, since these tunneling vectors might spontaneously break time-reversal symmetry.

As before, there are $(N-1)$ linearly independent tunneling vectors with $T = +\Sigma_1 T$, while the tunneling matrix \bar{T} from Eq. (3.12) must belong to any \mathbb{H} with N linearly independent tunneling vectors.

At this stage, we need to distinguish the case

$$\bar{T}^\top S = 0 \quad (3.17a)$$

from the case

$$\bar{T}^\top S \neq 0. \quad (3.17b)$$

In the former case, the spin neutrality condition (3.16b) holds for \bar{T} and thus the stability criterion is unchanged for the FQSHE. In the latter case, the spin neutrality condition (3.16b) is violated so that \hat{H}_{int} is independent of any tunneling matrix proportional to \bar{T} . Thus, when Eq. (3.17b) holds, as could be the case when $\kappa \propto \mathbb{1}_N$ and $\Delta = 0$ say, the FQSHE carried by at least one Kramers pair of edge states of \hat{H}_0 is robust to the strong coupling limit of the time-reversal symmetric and residual spin-1/2 $U(1)$ symmetric perturbation \hat{H}_{int} .

IV. SUMMARY

We have considered in this paper a subclass of time-reversal-symmetric fractional topological liquids without

quantized charge and spin Hall conductance. These states can be viewed as “zero filling fraction” quantum Hall states, that are related to an Abelian Chern-Simons bulk theory. The states we considered depart from previous constructions that place together two copies of FQHE systems, and as such they do not need to satisfy spin conservation or display quantized spin Hall conductances.

We have analyzed the stability of the edge theory associated with this type of state, and obtained a discriminant, the parity of an integer, that resolves whether there remains or not delocalized edge states in the presence of disorder. When the discriminant is even, there are no gapless edge modes. In contrast, gapless edge modes are protected by time-reversal symmetry when the discriminant is odd. These results contain as particular cases that display a quantized FQSHE,²⁰ where the discriminant has a relation to the then quantized spin Hall conductance.

We have also presented a concrete lattice realization of a FQSHE. There have been numerous studies on the effect of strong interactions in time-reversal symmetric systems with non-trivial topology at half filling.⁴⁶ In contrast, we have considered the effects of interactions at a partial filling of bands. At 2/3 filling of a lattice with 24 sites, exact diagonalization delivers a ground state with 9-fold degeneracy, which we interpret as a time-reversal-symmetric fractional topological liquid. We studied the stability of this phase by tuning parameters of the electron-electron interaction. In particular, we found a transition towards a phase of spontaneously broken time-reversal symmetry, which is related to a FQHE at 1/3 filling.

Let us remark that the lattice model presented in this paper is an example of fractionalization in two spatial dimensions without breaking time-reversal symmetry. It thus joins the ranks with the other known examples thereof constructed on lattices so far, that of electron-fractionalization in graphene-like systems in Refs. 47–50 together with the lattice gauge theory presented in Ref. 23, that of the triangular lattice quantum dimer model in Ref. 51, and that of the doubled chiral spin liquids in Ref. 52.

We would like to close this paper by spotlighting some perspectives on the differences between the \mathbb{Z}_2 topological band (weakly interacting) insulators and the time-reversal-symmetric fractional topological liquid states whose very existences are driven by interactions, in particular as to the importance that one should associate with the bulk and boundary states. In the case of the non-interacting (weakly-interacting) systems, the edge states play a disproportionally important role, in that the bulk states are just band insulators without any ground state degeneracy. On the other hand, the time-reversal-symmetric fractional topological liquids display quite rich bulk phenomena, including the possibility of fractionalized quasiparticles, regardless of whether gapless edge modes survive or not. Fractionalized particles can be probed without looking at the edge: capacitive

measurements in the bulk,⁵³ for instance, have revealed fractionalized electrons in the bulk of $\nu = 1/3$ FQH states. From this perspective, fractional time-reversal-symmetric topological liquid states should, as one might expect, be much richer in content than \mathbb{Z}_2 topological band (weakly-interacting) insulators.

ACKNOWLEDGMENTS

We gratefully acknowledge useful discussions with Rudolf Morf, Maurizio Storni, Xiao-Gang Wen, and Andrei Bernevig. We are indebted to Michael A. Levin for useful discussions regarding the FQSHE. In particular, we learned from Andrei Bernevig that he too is studying time-reversal-symmetric fractional topological liquids.⁵⁴ This work was supported in part by DOE Grant DEFG02-06ER46316. TN and CM thank the Condensed Matter Theory Visitors Program at Boston University for support.

Appendix A: Chiral bosonic quantum theory

In this Appendix, we review the construction of $2N$ Fermi-Bose and $2N$ quasi-particle vertex operators from the chiral bosonic quantum fields $\hat{\Phi}_i(t, x)$, $i = 1, \dots, 2N$, that enter the time-reversal invariant quantum edge theory with broken translation invariance (3.1) and discuss their universal properties. To this end, we consider the *universal data* (K, Q) entering the theory defined by Eq. (3.1) as opposed to the *non-universal data* $(V, h_T(x), \alpha_T(x))$.

On the chiral bosonic quantum fields we impose the boundary conditions

$$K_{ij} \hat{\Phi}_j(t, x + L) = K_{ij} \hat{\Phi}_j(t, x) + 2\pi n_i \quad (\text{A1})$$

with $n_i \in \mathbb{Z}$ for all $i = 1, \dots, 2N$. Together with the condition that the tunneling vectors T are restricted to have integer-valued components, this ensures that the Hamiltonian \hat{H} is single-valued.

The chiral nature of the bosonic quantum fields arises from demanding that the equal-time commutator

$$[\hat{\Phi}_i(t, x), \hat{\Phi}_j(t, x')] = -i\pi \left(K_{ij}^{-1} \text{sgn}(x - x') + \Theta_{ij} \right) \quad (\text{A2})$$

holds for any pair $i, j = 1, \dots, 2N$. Here,

$$\Theta_{ij} := K_{ik}^{-1} L_{kl} K_{lj}^{-1} \quad (\text{A3})$$

and antisymmetric $2N \times 2N$ matrix L is defined by (see Ref. 25)

$$L_{ij} = \text{sgn}(i - j) (K_{ij} + Q_i Q_j), \quad (\text{A4})$$

where $\text{sgn}(0) = 0$ is understood. It then follows that the quadratic theory (3.1b) is endowed with chiral equations

of motion. Finally, we need to impose the compatibility conditions

$$(-)^{K_{ii}} = (-)^{Q_i}, \quad i = 1, \dots, 2N, \quad (\text{A5})$$

in order to construct local excitations with well-defined statistics.

Define for any $i = 1, \dots, 2N$ the pair of normal-ordered vertex operators

$$\hat{\Psi}_{\text{q-p}, i}^\dagger(t, x) := : e^{-i\hat{\Phi}_i(t, x)} : \quad (\text{A6a})$$

and

$$\hat{\Psi}_{\text{f-b}, i}^\dagger(t, x) := : e^{-iK_{ij} \hat{\Phi}_j(t, x)} :, \quad (\text{A6b})$$

respectively. For any $i = 1, \dots, 2N$, the quasiparticle vertex operator $\hat{\Psi}_{\text{q-p}, i}^\dagger(t, x)$ is multi valued under the transformation (A13) provided $|\det K| > 1$ in contrast to the Fermi-Bose vertex operator $\hat{\Psi}_{\text{f-b}, i}^\dagger(t, x)$ which is always single valued under the transformation (A13).

For any pair $i, j = 1, \dots, N$, the equal-time commutator (3.1c) delivers the identities

$$[\hat{\mathcal{N}}_i, \hat{\Psi}_{\text{q-p}, j}^\dagger(t, x)] = \delta_{ij} \hat{\Psi}_{\text{q-p}, j}^\dagger(t, x), \quad (\text{A7a})$$

$$[\hat{\mathcal{N}}_i, \hat{\Psi}_{\text{f-b}, j}^\dagger(t, x)] = K_{ij} \hat{\Psi}_{\text{f-b}, j}^\dagger(t, x), \quad (\text{A7b})$$

and

$$[\hat{\mathcal{C}}_i, \hat{\Psi}_{\text{q-p}, j}^\dagger(t, x)] = K_{ij}^{-1} \hat{\Psi}_{\text{q-p}, j}^\dagger(t, x), \quad (\text{A8a})$$

$$[\hat{\mathcal{C}}_i, \hat{\Psi}_{\text{f-b}, j}^\dagger(t, x)] = \delta_{ij} \hat{\Psi}_{\text{f-b}, j}^\dagger(t, x), \quad (\text{A8b})$$

respectively. Here, the quasiparticle vertex operator $\hat{\Psi}_{\text{q-p}, i}^\dagger(t, x)$ is an eigenstate of the conserved topological number operator [recall Eq. (A1)]

$$\begin{aligned} \hat{\mathcal{N}}_i &:= \frac{1}{2\pi} K_{ij} \int_0^L dx \left(\partial_x \hat{\Phi}_j \right) (t, x) \\ &= \frac{1}{2\pi} K_{ij} \left[\hat{\Phi}_j(t, L) - \hat{\Phi}_j(t, 0) \right] \end{aligned} \quad (\text{A9a})$$

with eigenvalue one, while the Fermi-Bose vertex operator $\hat{\Psi}_{\text{f-b}, i}^\dagger(t, x)$ is an eigenstate of the conserved operator

$$\hat{\mathcal{C}}_i := \frac{1}{2\pi} \left[\hat{\Phi}_i(t, L) - \hat{\Phi}_i(t, 0) \right] \quad (\text{A9b})$$

with eigenvalue one for any $i = 1, \dots, 2N$.

The permutation statistics obeyed by any pair $i, j = 1, \dots, 2N$ of quasiparticle and Fermi-Bose operators follows from the application of the Baker-Campbell-Hausdorff formula,

$$\hat{\Psi}_{\text{q-p},i}^\dagger(t, x) \hat{\Psi}_{\text{q-p},j}^\dagger(t, x') = \hat{\Psi}_{\text{q-p},j}^\dagger(t, x') \hat{\Psi}_{\text{q-p},i}^\dagger(t, x) e^{-i\pi [K_{ji}^{-1} \text{sgn}(x-x') + \Theta_{ij}]} \quad (\text{A10a})$$

and

$$\hat{\Psi}_{\text{f-b},i}^\dagger(t, x) \hat{\Psi}_{\text{f-b},j}^\dagger(t, x') = \hat{\Psi}_{\text{f-b},j}^\dagger(t, x') \hat{\Psi}_{\text{f-b},i}^\dagger(t, x) e^{-i\pi [K_{ij} \text{sgn}(x-x') + L_{ij}]} \quad (\text{A10b})$$

when $x \neq x'$, respectively. We conclude that, for any $x \neq x'$, demanding that the $2N \times 2N$ matrix K and the $2N$ -component charge vector Q are integer-valued together with the compatibility condition (A5) is required to obtain local excitations carrying the Fermi-Bose permutation statistics

$$\hat{\Psi}_{\text{f-b},i}^\dagger(t, x) \hat{\Psi}_{\text{f-b},j}^\dagger(t, x') = (-1)^{Q_i Q_j} \hat{\Psi}_{\text{f-b},j}^\dagger(t, x') \hat{\Psi}_{\text{f-b},i}^\dagger(t, x). \quad (\text{A10c})$$

Let us now deduce the connection between the charge vector Q , the conserved operators \hat{C}_i , and the total charge density operator \hat{Q} that follows from integrating Eq. (3.1e) along the edge. The charge vector Q enters explicitly the theory after coupling the $2N$ chiral scalar fields to an external vector gauge potential with the components A_0 and A_1 through the minimal coupling. The minimal coupling consists in replacing the x derivative by the covariant derivative

$$\partial_x \hat{\Phi}_i \rightarrow D_x \hat{\Phi}_i := (\partial_x + Q_i A_1) \hat{\Phi}_i, \quad (\text{A11a})$$

for $i = 1, \dots, 2N$ and adding the contribution

$$\hat{H}_{\text{current}} := \int_0^L dx \frac{1}{2\pi} A_0 (Q^\top D_x \hat{\Phi}) \quad (\text{A11b})$$

on the right-hand side of Eq. (3.1a). The theory is then invariant under the pure $U(1)$ electro-magnetic gauge transformation

$$\hat{\Phi} \rightarrow \hat{\Phi} + Q\chi, \quad A_1 \rightarrow A_1 - \partial_x \chi. \quad (\text{A11c})$$

We can now define the total charge operator by

$$\hat{Q} := Q_i \mathcal{C}_i. \quad (\text{A12})$$

It follows that the charge associated with the quasiparticle operator $\hat{\Psi}_{\text{q-p},i}^\dagger$ and with the Fermi-Bose operator $\hat{\Psi}_{\text{f-b},i}^\dagger$ is given by $K_{ij}^{-1} Q_j$ and Q_i , respectively.

By assumption, the integer-valued $2N \times 2N$ matrix K is symmetric and invertible. Consequently, its inverse K^{-1} is also symmetric, but its matrix elements are rational numbers whenever $|\det K| > 1$. Observe that the model (3.1) is invariant under the transformation

$$\hat{\Phi}(t, x) \rightarrow \hat{\Phi}(t, x) + 2\pi T_* \quad (\text{A13a})$$

for any $T_* \in \mathbb{R}^{2N}$ that is independent of space and time and such that

$$T^\top K T_* \in \mathbb{Z}, \quad Q^\top T_* = 0, \quad (\text{A13b})$$

for all tunneling vectors $T \in \mathbb{L}$. The quantum Hamiltonian (3.1) thus possesses an emergent global $(U(1))^{2N}$ symmetry compared to the microscopic model. The set of all rational-valued vectors T_* that satisfy conditions (A13) is the lattice \mathbb{L}^* dual to the lattice \mathbb{L} . When $|\det K| > 1$, the lattice \mathbb{L} is a sublattice of the dual lattice \mathbb{L}^* that is generated by the quasiparticles carrying a unit topological charge. The ground state of Hamiltonian (3.1) with the periodic boundary conditions corresponding to the geometry of a torus is then degenerate with the degeneracy $|\det K| > 1$, which is nothing but the volume of the unit cell of the lattice \mathbb{L} in units of the unit cell of the dual lattice \mathbb{L}^* .

Note that there is no unique way to define the dual pair \mathbb{L} and \mathbb{L}^* . For example, we can use Eq. (A7a) to define the dual lattice \mathbb{L}^* to be based on the hypercubic lattice \mathbb{Z}^{2N} and, in turn, use Eq. (A13b) to construct \mathbb{L} . Alternatively, we can use Eq. (A8b) to define the lattice \mathbb{L} to be based on the hypercubic lattice \mathbb{Z}^{2N} and, in turn, use Eq. (A13b) to construct the dual lattice \mathbb{L}^* . Either ways, the ratio between the unit cells of the lattices \mathbb{L} and \mathbb{L}^* is $|\det K|$. We have chosen the latter option.

Appendix B: Non-interacting fermionic edge theory with time-reversal symmetry

In this Appendix, we review a non-interacting fermionic theory to analyze the role of disorder on the edge of a two-dimensional band insulator when imposing time-reversal symmetry. We consider a cylindrical geometry as is depicted in Fig. 2. If the length L_y of the cylinder is much larger than the characteristic linear extension into the bulk of edge states, the two edges at $y = \pm L_y/2$ decouple. The low-energy and long-wave-length random single-particle Hamiltonian that describes any one of the two edges, each supporting N Kramers degenerate pairs

of electrons, is then given by

$$\begin{aligned}\mathcal{H}(x) &:= i v_F \sigma_3 \otimes \mathbb{1}_N \partial_x + \mathcal{W}(x) = \mathcal{T}^{-1} \mathcal{H}(x) \mathcal{T}, \\ \mathcal{W}(x) &:= \sum_{\mu=0}^3 \sigma_\mu \otimes W_\mu(x) = \mathcal{T}^{-1} \mathcal{W}(x) \mathcal{T},\end{aligned}\quad (\text{B1a})$$

where the operation of time-reversal for spin-1/2 electrons is represented by

$$\mathcal{T} := i \sigma_2 \mathcal{K} = -\mathcal{T}^\top \quad (\text{B1b})$$

(\mathcal{K} represents the operation of charge conjugation). Here, we have introduced the unit 2×2 matrix σ_0 and the three Pauli matrices σ_1 , σ_2 , and σ_3 . In view of Eq. (B1b), σ_1 , σ_2 , and σ_3 are to be interpreted as the generators of the spin-1/2 algebra of the electrons. The matrix $\mathbb{1}_N$ is the unit $N \times N$ matrix. The matrix elements of the $N \times N$ Hermitean matrices $W_\mu(x)$ with $\mu = 0, 1, 2, 3$ must obey

$$\begin{aligned}W_0(x) &= +W_0^*(x), & W_1(x) &= -W_1^*(x), \\ W_2(x) &= -W_2^*(x), & W_3(x) &= -W_3^*(x),\end{aligned}\quad (\text{B1c})$$

for time-reversal symmetry to hold. Hence, they can be taken as random numbers obeying the white-noise and Gaussian distribution of mean

$$\langle (W_\mu)_{ij}(x) \rangle = v_i \delta_{ij} \delta_{\mu,3}, \quad (\text{B1d})$$

and co-variance

$$\begin{aligned}\langle (W_\mu)_{ij}(x) (W_\nu^*)_{kl}(x') \rangle &= \frac{1}{N\ell} \left(\delta_{ik} \delta_{jl} - (-)^{\delta_{\mu,0}} \delta_{il} \delta_{jk} \right) \\ &\quad \times \delta_{\mu\nu} \delta(x - x'),\end{aligned}\quad (\text{B1e})$$

with $i, j = 1, \dots, N$ the flavor index that label the Kramers degenerate pairs of electrons. The length scale ℓ is the mean free path within the Born approximation. The channel $\mu = 3$ represents forward scattering and the mean v_i for $i = 1, \dots, N$ results, through a gauge transformation, in a flavor-dependent shift of the Fermi velocity v_F .

It was known from the studies of quasi-one-dimensional wires in the 1980's that the random potential $\mathcal{W}(x)$ localizes all N Kramers degenerate pairs of electrons when N is even.⁵⁵ It was only realized with the seminal work of Ando and Suzuura in Ref. 56 on carbon nanotubes that the case of an odd number N is (i) of physical relevance

and (ii) only localizes $(N-1)$ Kramers degenerate pairs of electrons, leaving one pair delocalized along the edge.⁵⁷ It then took two groundbreaking papers from Kane and Mele on graphene with spin-orbit coupling to make the deep connection that this absence of Anderson localization is the essence of a two-dimensional \mathbb{Z}_2 topological insulator.^{12,13}

Observe that the integer quantum spin Hall effect (IQSHE) can be deduced from the following special case of Eq. (B1). If we demand that the symmetry condition

$$\sigma_3 \mathcal{H}(x) \sigma_3 = \mathcal{H}(x) \quad (\text{B2a})$$

also holds in addition to the time-reversal symmetry in Eq. (B1). Condition (B2a) is then nothing but the residual spin-1/2 U(1) symmetry generated by rotations about the spin-1/2 quantization axis σ_3 . Imposing the residual spin-1/2 U(1) symmetry (B2a) on the disorder potential $\mathcal{W}(x)$ amounts to the restrictions

$$W_1(x) = W_2(x) = 0 \quad (\text{B2b})$$

for all x along the edge. Condition (B2b) removes all backward scattering channels from the single-particle disorder potential $\mathcal{W}(x)$. The single-particle Hamiltonian $\mathcal{H}(x)$ thus decomposes into the direct sum of two Hamiltonians, each of which realizes an integer quantum Hall edge, but with opposite quantized Hall conductivity of magnitude N in units of e^2/h . The difference between these quantized Hall conductivities is proportional to N and yields the quantized spin Hall conductivity $2N$ in units of $e/(4\pi)$.

In Sec. III, we consider an interacting effective quantum field theory including local multi-particle interactions that break translation invariance. The only allowed *underlying microscopic* symmetries of this interacting effective quantum field theory are charge conservation and time-reversal symmetry. The time-reversal symmetry in Sec. III, in particular Eqs. (3.3d) and (3.3e), are inherited from the following properties of the single-particle disorder potential in Eq. (B1a). If A is any complex-valued matrix, denote with $\text{abs}(A)$ and $\text{arg}(A)$ the matrices with the matrix elements given by the absolute values and phases of the entries in A , respectively. One then verifies that

$$\begin{aligned}\text{abs}(\Sigma_1 \mathcal{W}(x) \Sigma_1) &= \text{abs} \mathcal{W}(x), \\ \text{arg}(\Sigma_1 \mathcal{W}(x) \Sigma_1) &= \pi \sigma_1 \otimes E - \text{arg} \mathcal{W}(x),\end{aligned}\quad (\text{B3})$$

where E is the $N \times N$ matrix with one for all matrix elements.

¹ K. v. Klitzing, G. Dorda, and M. Pepper, Phys. Rev. Lett. **45**, 494 (1980).

² R. B. Laughlin Phys. Rev. B **23**, 5632 (1981)

³ B. I. Halperin, Phys. Rev. B **25**, 2185 (1982).

⁴ D. C. Tsui, H. L. Stormer, and A. C. Gossard, Phys. Rev.

Lett. **48**, 1559 (1982).

⁵ H. L. Stormer, A. Chang, D. C. Tsui, J. C. Hwang, A. C. Gossard, and W. Wiegmann, Phys. Rev. Lett. **50**, 1953 (1983).

⁶ R. B. Laughlin, Phys. Rev. Lett. **50**, 1395 (1983).

- ⁷ F. D. M. Haldane, Phys. Rev. Lett. **51**, 605 (1983).
⁸ X.-G. Wen, Int. J. Mod. Phys. B **4**, 239 (1990).
⁹ X.-G. Wen, Phys. Rev. Lett. **64**, 2206 (1990).
¹⁰ X.-G. Wen, Phys. Rev. B **43**, 11025 (1991).
¹¹ X.-G. Wen, Phys. Rev. B **44**, 5708 (1991).
¹² C. L. Kane and E. J. Mele, Phys. Rev. Lett. **95**, 226801 (2005).
¹³ C. L. Kane and E. J. Mele, Phys. Rev. Lett. **95**, 146802 (2005).
¹⁴ B. A. Bernevig and S.-C. Zhang, Phys. Rev. Lett. **96**, 106802 (2006).
¹⁵ B. A. Bernevig, T. L. Hughes, and S.-C. Zhang, Science **314**, 1757 (2006).
¹⁶ M. König, S. Wiedmann, C. Brüne, A. Roth, H. Buhmann, L. W. Molenkamp, X.-L. Qi, and S.-C. Zhang, Science **318**, 766 (2007).
¹⁷ F. D. M. Haldane, Phys. Rev. Lett. **61**, 2015 (1988).
¹⁸ M. Freedman, C. Nayak, K. Shtengel, K. Walker, and Z. Wang, Ann. of Phys. (N.Y.) **310**, 428 (2004).
¹⁹ T. H. Hansson, V. Oganesyan, and S. L. Sondhi, Ann. Phys. **313**, 497 (2004).
²⁰ M. Levin and A. Stern, Phys. Rev. Lett. **103**, 196803 (2009).
²¹ J. Fröhlich, F. Gabbiani, and P. Marchetti, *Braid statistics in three-dimensional local quantum theory in Physics, Geometry and Topology*, Editor: H. Lee, Plenum Press, New York, 1990.
²² G. Moore and N. Read, Nucl. Phys. B **360**, 362 (1991).
²³ S. Ryu, C. Mudry, C.-Y. Hou, and C. Chamon, Phys. Rev. B **80**, 205319 (2009).
²⁴ More precisely, to guarantee that there are N_K Kramers degenerate pairs of electrons in the theory, we demand that there exists a space and time independent transformation

$$O = +\Sigma_1 O \Sigma_1 \in \text{GL}(2N, \mathbb{Z})$$
such that

$$K \rightarrow O^\top K O, \quad V \rightarrow O^\top V O,$$
and

$$Q \rightarrow O Q$$
with the transformed charge vector containing $2N_K$ odd integers.
²⁵ F. D. M. Haldane, Phys. Rev. Lett. **74**, 2090 (1995).
²⁶ C. L. Kane, M. P. A. Fisher, and J. Polchinski, Phys. Rev. Lett. **72**, 4129 (1994).
²⁷ J. E. Moore and X.-G. Wen, Phys. Rev. B **57**, 10 138 (1998).
²⁸ J. D. Naud, L. P. Pryadko, and S. L. Sondhi, Nucl. Phys. B **565**, 572 (2000).
²⁹ J. D. Naud, L. P. Pryadko, and S. L. Sondhi, Phys. Rev. B **63**, 115301 (2001).
³⁰ T. Neupert, L. Santos, C. Chamon, and C. Mudry, Phys. Rev. Lett. **106**, 236804 (2011).
³¹ D. N. Sheng, Z. Gu, K. Sun, and L. Sheng, arXiv:1102.2658 (unpublished).
³² Y.-F. Wang, Z.-C. Gu, C.-D. Gong, D. N. Sheng, arXiv:1103.1686 (unpublished).
³³ N. Regnault and B. A. Bernevig, arXiv:1105.4867 (unpublished).
³⁴ E. Tang, J.-W. Mei, and X.-G. Wen, Phys. Rev. Lett. **106**, 236802 (2011).
³⁵ K. Sun, Z. Gu, H. Katsura, and S. Das Sarma, Phys. Rev. Lett. **106**, 236803 (2011).
³⁶ D. Green, L. Santos, and C. Chamon, Phys. Rev. B **82**, 075104 (2010).
³⁷ X.-L. Qi, arXiv:1105.4298 (unpublished).
³⁸ S. Parameswaran, R. Roy, and S. Sondhi, arXiv:1106.4025 (unpublished).
³⁹ D. Xiao, W. Zhu, Y. Ran, N. Nagaosa, and S. Okamoto, arXiv:1106.4296 unpublished.
⁴⁰ A. P. Schnyder, S. Ryu, A. Furusaki, and A. W. W. Ludwig, Phys. Rev. B **78**, 195125 (2008).
⁴¹ A. Kitaev, AIP Conf. Proc. **1134**, 22 (2009).
⁴² S. Ryu, A. P. Schnyder, A. Furusaki, and A. W. W. Ludwig, New J. Phys. **12**, 065010 (2010).
⁴³ L. Santos, T. Neupert, S. Ryu, C. Chamon, and C. Mudry, (in preparation).
⁴⁴ C. Xu and J. E. Moore, Phys. Rev. B **73**, 045322 (2006).
⁴⁵ It is important to observe that the quadratic Hamiltonian (3.1a) has a much larger symmetry group than the interacting Hamiltonian (3.1f). For example, \hat{H}_0 commutes with the transformation

$$\hat{\Phi}(t, x) \longrightarrow \hat{\Phi}(t, x) + \pi K^{-1} \Sigma_\downarrow S.$$
One verifies that the transformation law of a Kramers doublet of fermions under this transformation is the one expected from a rotation about the quantization axis of the residual spin-1/2 U(1) symmetry provided the parities of the components of S are the same as those of Q . Hence, \hat{H}_0 has, by construction, the residual spin-1/2 U(1) symmetry even though a generic microscopic model with time-reversal symmetry does not. This residual spin-1/2 U(1) symmetry of \hat{H}_0 is broken by \hat{H}_{int} , unless one imposes the additional constraint (3.16b) on the tunneling matrices $T \in \mathbb{L}$ allowed to enter the interacting theory defined in Eq. (3.1).
⁴⁶ S. Raghu, X.-L. Qi, C. Honerkamp, and S.-C. Zhang, Phys. Rev. Lett. **100**, 156401 (2008); K. Sun, H. Yao, E. Fradkin, and S. A. Kivelson, Phys. Rev. Lett. **103**, 046811 (2009); Y. Zhang, Y. Ran, and A. Vishwanath, Phys. Rev. B **79**, 245331 (2009); L. Fidkowski and A. Kitaev, Phys. Rev. B **81**, 134509 (2010); J. Wen, A. Rüegg, C. J. Wang, and G. A. Fiete, Phys. Rev. B **82**, 075125 (2010); M. Dzero, K. Sun, V. Galitski, and P. Coleman, Phys. Rev. Lett. **104**, 106408 (2010); D. Pesin and L. Balents, Nat. Phys. **6**, 376 (2010); C. N. Varney, K. Sun, M. Rigol, and V. Galitski, Phys. Rev. B **82**, 115125 (2010); S. Rachel and K. Le Hur, Phys. Rev. B **82**, 075106 (2010); D. Soriano and J. Fernández-Rossier, Phys. Rev. B **82**, 161302 (2010); M. Hohenadler, T. C. Lang, and F. F. Assaad, Phys. Rev. Lett. **106**, 100403 (2011); J. Goryo and N. Maeda, arXiv:1007.4671 (unpublished); D. Zheng, C. Wu, and G.-M. Zhang, arXiv:1011.5858 (unpublished); D.-H. Lee, arXiv:1105.4900 (unpublished), A. Rüegg and G. A. Fiete, arXiv:1106.1559 (unpublished).
⁴⁷ C.-Y. Hou, C. Chamon, and C. Mudry, Phys. Rev. Lett. **98**, 186809 (2007).
⁴⁸ R. Jackiw and S.-Y. Pi, Phys. Rev. Lett. **98**, 266402 (2007).
⁴⁹ C. Chamon, C.-Y. Hou, R. Jackiw, C. Mudry, S.-Y. Pi, and A. P. Schnyder, Phys. Rev. Lett. **100**, 110405 (2008).
⁵⁰ C. Chamon, C.-Y. Hou, R. Jackiw, C. Mudry, S.-Y. Pi, and G. Semenoff, Phys. Rev. B **77**, 235431 (2008).
⁵¹ R. Moessner and S. L. Sondhi, Phys. Rev. Lett. **86**, 1881 (2001).
⁵² B. Scharfenberger, R. Thomale, and M. Greiter, arXiv:1105.4348 (unpublished).
⁵³ J. Martin, S. Ilani, B. Verdene, J. Smet, V. Umansky, D.

- Mahalu, D. Schuh, G. Abstreiter, and A. Yacoby, *Science* **305**, 980 (2004).
- ⁵⁴ Andrei Bernevig et al., private communication.
- ⁵⁵ For a review, see C. W. J. Beenakker, *Rev. Mod. Phys.* **69**, 731 (1997).
- ⁵⁶ T. Ando and H. Suzuura, *J. Phys. Soc. Jpn.* **71**, 2753 (2002).
- ⁵⁷ Y. Takane, *J. Phys. Soc. Jpn.* **73**, 9 (2004); 1430 (2004); 2366 (2004).